Journal of Alloys and Compounds 509 (2011) 9190–9194

Contents lists available at ScienceDirect

Journal of Alloys and Compounds

journal homepage: www.elsevier.com/locate/jallcom

Electrocatalytic behaviour of NiBi coatings for hydrogen evolution reaction in alkaline medium

Mehmet Erman Mert, Gülfeza Kardaş*

Çukurova University, Science and Letters Faculty, Chemistry Department, 01330 Balcalı, Adana, Turkey

ARTICLE INFO

Article history:
Received 6 May 2011
Received in revised form 27 June 2011
Accepted 27 June 2011
Available online 2 July 2011

Keywords:
Catalysis
Coating materials
Scanning electron microscopy
Energy dispersive X-ray

ABSTRACT

The nickel–bismuth binary coatings with various chemical compositions were galvanostatically deposited on the copper electrode in view of their possible applications as electrocatalytic materials for the hydrogen evolution reaction (HER) in alkaline solution. The HER activity of coatings was tested with the help of potentiodynamic measurements and electrochemical impedance spectroscopy (EIS) technique. The electrochemical characterization was achieved by the means of cyclic voltammetry (CV). The surface morphology and surface composition of coatings were determined with scanning electron microscopy (SEM), and energy dispersive X-ray (EDX). The potentiodynamic measurements show that, the binary coatings decrease the hydrogen over potential and increase the current density values for HER. The EIS analysis confirms, the charge transfer resistances decrease and the double layer capacitance values increase for binary coatings. The EDX results in sign that the composition of binary coating changes by using coating bath. The Cu/NiBi-2 coating (Ni^{2+}/Bi^{3+} is 99.71:0.29 molar ratio) is the best suitable cathode composition for the HER in alkaline media under these experimental conditions.

1. Introduction

The energy consumption has been increased parallel with increasing world population and technological developments. Due to the rapid depletion of fossil fuels, intensive research works have been done to search for new and alternative energy sources. Hydrogen is considered an ideal energy carrier that can be an alternative to fossil fuels [1,2]. Hydrogen is very popular for a number of reasons: it is perceived as a clean fuel because, the reaction of hydrogen with oxygen produces the water vapor which is not an atmosphere pollutant [3]; it can be produced using any energy sources, with renewable energy being most attractive; it works with fuel cells and together, it may serve as one of the solutions to the sustainable energy supply [4–7]. It is produced by the means of gasification [8,9], biochemical process [10,11] and electrolysis techniques [12–16]. The gasification realizes between the range of 800–2000 °C and 40 atm a pressure also process efficiency is 55% that low reaction completion grade. Despite the biochemical processes' high costs and complex device requirements researches are being continued on, but still not acceptable for applications [17]. Electrolysis is the more favorable and efficient production process of hydrogen without any environmental problems. The main disadvantage of this method is energy consumption, but it can solve with solar energy, etc. systems. The idea is; solar energy can be use due to the source at electrolysis cell and the evaluated hydrogen gas can be stored using several methods and phenomena: compressed hydrogen in high-pressure gas cylinders; liquid hydrogen in cryogenic tanks; adsorbed hydrogen on materials with a large specific surface area; absorbed on interstitial sites in a host metal and it is used whenever energy needs [3,18–21].

The research and development efforts have been recently focused on the minimizing ohmic drop, lowering the overpotential through the improvement of the cell and electrode design and using new and cheaper cathode materials with higher electrocatalytic activity for the hydrogen evolution reaction (HER) [22–26]. These electrodes are usually made of Ni, Co, V, Mo, etc. composite coatings or alloys considering the desirable relation between their electrocatalytic properties towards hydrogen production, corrosion resistance to the strongly alkaline environment [26–31]. Especially the nickel-based coating materials have been widely studied since past decades, which lead to the conclusion that the film properties are strongly influenced by deposition techniques and condition [32]. Results show that, the trace amount of metal additives in Ni plating bath, improves the properties of coating and enhances surface roughness and catalytic activity [33,34]. For this purpose, bismuth should be convenient additive due to its unique physical and chemical properties. It has been widely used in many areas: (1) electrochromic material, (2) alternative to mercury film electrode in electroanalysis, (3) magneto resistance or thermoelectric applications, etc. [35–39]. But the electrocatalytic activity of the nickel–bismuth binary coatings for the HER has not been reported yet. The aim of this study is electrochemical preparation

* Corresponding author. Tel.: +90 322 338 60 81; fax: +90 322 338 60 70.
E-mail address: gulfeza@cu.edu.tr (G. Kardaş).

0925-8388/$ – see front matter © 2011 Elsevier B.V. All rights reserved.
doi:10.1016/j.jallcom.2011.06.107

and characterization of the NiBi coatings in view of their possible applications as electrocatalytic materials for the HER in the alkaline medium.

2. Experimental

The copper electrodes were cut from a cylindrical rod to a length of 5 cm and coated with polyester to a surface area of 0.283 cm^2. The electrical conductivity was provided by a copper wire. Before electrochemical measurements, the electrode surface was polished with emery paper (320–1200 grain size), then washed with distilled water, thoroughly degreased with acetone, washed once more with distilled water and immersed in a bath solution. The electrodeposition was performed galvanostatically using Ivium Stat electrochemical analyzer (serial number A06063) under computer control, with a three-electrode configuration. A nickel electrode was used as a counter electrode, Ag/AgCl electrode was used as the reference electrode. The composition of (a) nickel plating bath; %30 $NiSO_4{\cdot}7H_2O$, %1 $NiCl_2{\cdot}6H_2O$, %1.25 H_3BO_3, pH 5.6–6.2, (b) bismuth plating bath; 0.1 M $Bi(NO_3)_3{\cdot}5H_2O$ and 0.1 M tartaric acid ($C_4H_6O_6$) containing1 M HNO_3 (pH 1.7–2.0), (c) nickel–bismuth plating bath: the nickel and bismuth salts, which were used in the nickel and bismuth baths, were fixed in different molar ratios containing 1.25% H_3BO_3, whereas the total molar concentration of Ni^{2+} and Bi^{3+} was constant in all plating baths (1.11 M). The molar ratio of Ni^{2+}/Bi^{3+} in the plating bath was 99.6:0.4 (NiBi-1), 99.5:0.5 (NiBi-2), 99.4:0.6 (NiBi-3) and 99.3:0.7 (NiBi-4). The constant current density of 50 mA cm^{-2} was applied during the electrodeposition. The operation time was calculated via Faraday's laws of 10 mm film thickness.

The electrochemical measurements were carried out using a CHI 604D electrochemical analyzer (Serial Number R0633) under computer control with a three-electrode configuration. A platinum sheet (with 2 cm^2 surface area) and Ag/AgCl electrode were used as the auxiliary and the reference electrodes, respectively. The current–potential curves were obtained in the potential ranges between −1.0 and −1.8 V with a scan rate of 0.005 Vs^{-1}. The EIS experiments were conducted in the frequency range of 100–0.01 kHz at different potentials: −1.4, −1.5 and −1.6 V, the amplitude was 0.005 V. The EIS data were fitted using a ZWiev2 fitting program. The CV measurements were obtained in the potential ranges between −1.4 and 0.7 V with a scan rate of 0.1 Vs^{-1}. The SEM images were taken using a Carl Zeiss Leo 440 SEM instrument at high vacuum and 10 kV EHT, system was equipped with an energy dispersive X-ray (EDX) spectrometer.

3. Results and discussion

3.1. Electrochemical measurements

The potentiodynamic measurements were performed in 1 M KOH solution, with the scan rate of 0.005 Vs^{-1}. The recorded data are presented as cathodic current density (I_c) and potential (E) in Fig. 1. As it is seen from Fig. 1, from −1.0 V to −1.2 V, all the curves are similar and the current passing through the system is almost zero. Up to this potential, there is a rapid increase in the cathodic current with increasing applied potential due to the evolution of hydrogen at the cathode. In Fig. 1 the binary coatings were considerably higher current values in comparison to the Ni coated copper electrode, whereas their (Cu/NiBi-1; 2; 3; 4) activity was dependent upon the composition of the plating bath. The Cu/NiBi-2 electrode was convenient by the side of the other binary coatings (Fig. 1).

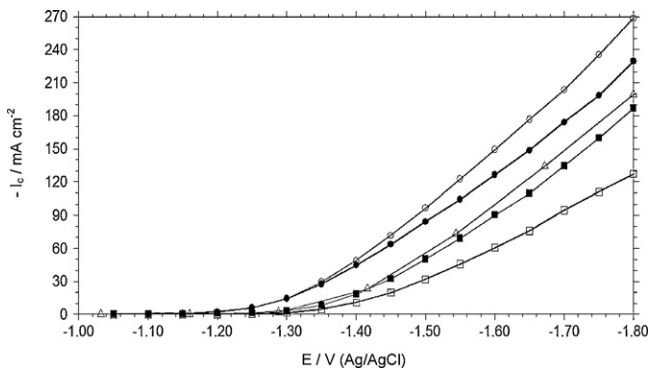

Fig. 1. The cathodic current–potential curves of working electrodes: Cu/Ni (□), Cu/NiBi-1 (●), Cu/NiBi-2 (o), Cu/NiBi-3 (△), Cu/NiBi-4 (■), recorded in 1 M KOH.

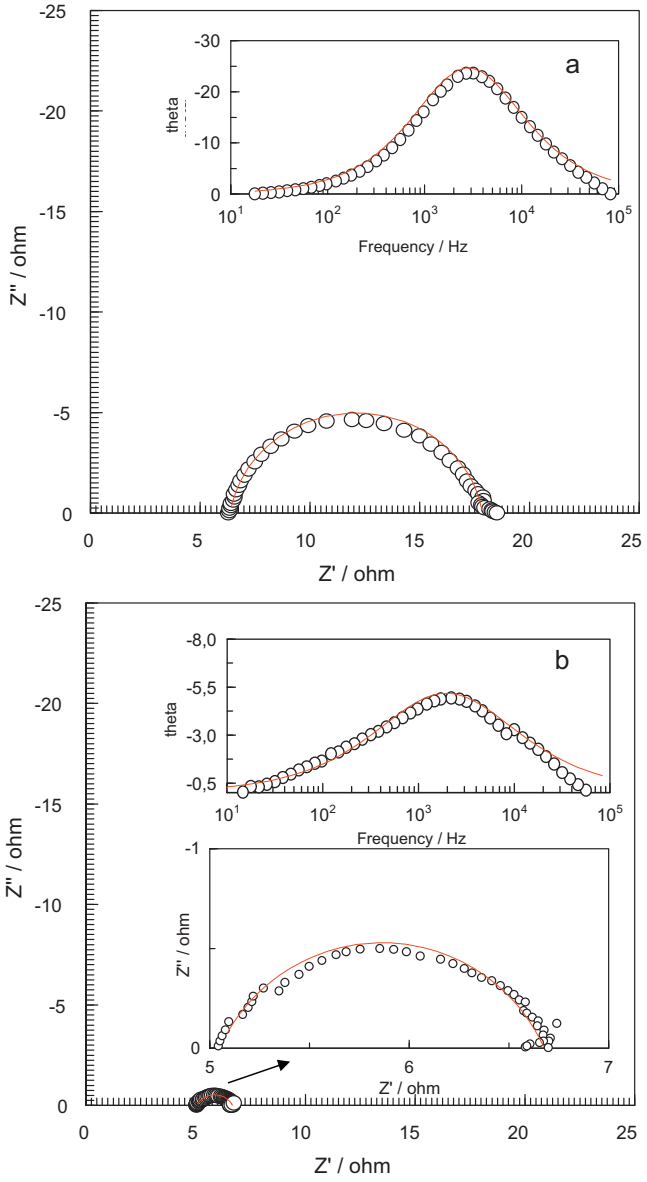

Fig. 2. Nyquist and frequency-phase angle (θ) diagrams of Cu/Ni (a), Cu/NiBi-2 (b) electrodes at −1.5 V in 1 M KOH solution: frame circles and solid lines represents experimental and fitted results respectively.

In order to compare the HER activity of these electrodes, EIS measurements were recorded at different potentials (−1.4, −1.5 and −1.6 V). The data which were obtained at −1.5 V, were presented in Fig. 2 for Cu/Ni and Cu/NiBi-2 electrodes. The EIS data were fitted according to the electrical equivalent circuit diagram given Fig. 3 and the calculated values were given in Table 1. In Fig. 2, the slightly depressed semi-circular shape with a diameter of 11.47 Ω, was observed in the Nyquist plot of Cu/Ni and obviously depressed semi-circular shape with a diameter of 1.63 Ω was observed in the Nyquist plot of Cu/NiBi-2. A single semi-circle was also found by other authors for the different electrodes [1,33,40,41].

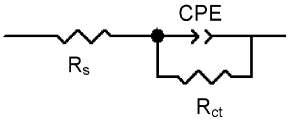

Fig. 3. Schematic representation of the electrical equivalent circuit diagram.

Table 1
Electrochemical parameters determined from the EIS measurements.

Coating	E/V	R_s/Ω	R_{ct}/Ω	CPE × 10^{-6}/μF cm^{-2}	n	R_f
Ni	−1.4	6.5	16.22	14.81	0.95	0.99
	−1.5	6.4	11.47	19.75	0.91	1.71
	−1.6	6.5	8.48	22.44	0.90	2.04
NiBi-1	−1.4	6.1	3.13	3254	0.61	10.59
	−1.5	5.8	2.38	4930	0.58	12.48
NiBi-2	−1.4	4.9	2.49	4305	0.65	21.95
	−1.5	5.1	1.63	7025	0.63	30.44
NiBi-3	−1.4	5.9	6.44	101	0.95	3.44
	−1.5	5.7	3.31	127	0.91	2.97
	−1.6	5.7	2.11	187	0.85	2.41
NiBi-4	−1.4	5.7	12.48	518	0.64	1.80
	−1.5	5.8	4.29	497	0.60	0.51
	−1.6	5.9	3.05	828	0.60	0.95

The observation of only semi-circular shape in the Nyquist plots indicates that the hydrogen evolution reaction is mainly controlled by a charge transfer process [2,33,40]. In Fig. 2 the maximum phase angle values were 28° and 5.7° for Cu/Ni and Cu/NiBi-2 electrodes, respectively. It is related to the surface in-homogeneities of the coatings [42,43]. The phase angle values show that, Cu/NiBi-2's surface is rougher than Cu/Ni surface's. It leads a high surface area available for the HER [40–43]. In addition it is a sign of the deviation from the ideal semi-circle. Therefore, a constant phase element (CPE) was used for fitting EIS results, in place of a double layer capacitance (C_{dl}), in order to give a more accurate fit to the experimental results. Generally, the use of a CPE is required due to the distribution of the relaxation times as a consequence of in-homogeneities present at a micro- or nano-level, such as the surface roughness/porosity, adsorption, or diffusion [44–46]. In Table 1, the CPE increase in the case of the binary coatings was related to the onset of the Faradaic reaction of the HER, which indicates the increasing electrocatalytic activity of the coatings [42,47]. It can be seen from Table 1, the parameter n, generally accepted to be a measure of surface inhomogeneity [42], was lower than 1.0, which indicates that the deposited coatings had a porous structure. Furthermore, the surface roughness factor (R_f) was calculated as the following equations [42,43];

$$C_{dl} = \frac{\text{CPE}.\omega(n-1)}{(\sin n\pi/2)} \quad (1)$$

$$R_f = \frac{C_{dl}}{20\mu\text{F cm}^{-2}} \quad (2)$$

where ω is angular frequency, and C_{dl} is the double layer capacitance. The C_{dl} was assumed 20 μF cm^2 for the smooth polycrystalline nickel electrode.

The calculated R_f values were given in Table 1. It was defined as the ratio of the real and the macroscopic areas. The $R_f = 1$ limiting case corresponds to the ideally smooth (e.g., single crystalline or liquid) surfaces, whereas $R_f = \infty$ (in reality, $R_f \gg 1$) holds if the electrode is of spongy, porous, three-dimensional structure [43,48]. The significant differences were existed between the values of R_f for Ni and NiBi-2 coatings (Table 1).

In Table 1, the charge transfer resistance of the binary coatings was lower than Ni coating. The Cu/NiBi-2 electrode has the lowest charge transfer resistance. The binary coating effect can be explained by a synergistic combination of the electrocatalytic components or by increasing the ratio between the real and geometric surface area of the electrode [32,41–48]. It has been previously reported that alloying the left-hand side transition metals (e.g., Fe, Co, Ni, etc.) with the right-half transition metals (e.g., Pt, Ag, Bi, etc.) results in significant changes to their bonding strength and consequently, increased inter metallic stability, whose maximum usually coincides with optimal d-electrons for the synergism and maximal activity in the HER [49–51].

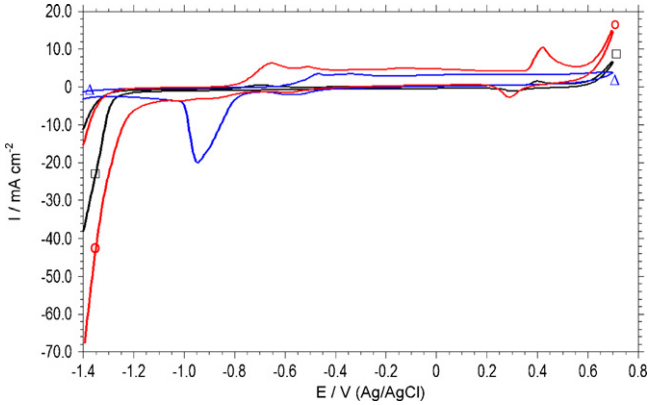

Fig. 4. The cyclic voltammograms of Cu/Ni (□), Cu/Bi (△), Cu/NiBi-2 (o) electrodes recorded in 1 M KOH solution.

3.2. Characterization of coatings

The surface morphologies of Cu/Ni, Cu/Bi and Cu/NiBi-2 electrodes were characterized with CV, SEM and EDX techniques. The CV is an easy way for the characterization of electrochemically deposited thin metallic coatings. The distribution of voltammetric peaks at different potentials is characteristic of each metal component because the number and the peak potentials depend only on the metal structure. The CVs of the Cu/Ni, Cu/Bi and Cu/NiBi-2 electrodes were obtained in 1 M KOH solution at 298 K between the hydrogen and oxygen evolution potential range, and the diagrams obtained are presented in Fig. 4. For Cu/Ni electrode, the peak at −0.68 V, corresponds to Ni/Ni^{2+} oxidation, the transformation of α-Ni(OH)$_2$ to β-Ni(OH)$_2$ takes place between the potential ranges of −0.57–0.34 V [26,52,53]. The peak centered at 0.41 V corresponds to the Ni^{2+}/Ni^{3+} transition [52,53]. The cathodic peak at 0.31 V, corresponds to the Ni^{3+}/Ni^{2+} reduction. The CV of the Cu/Bi electrode indicates that the peak at −0.47 V, corresponds to Bi/Bi^{3+} oxidation. During the anodic scan, the anodic current values were increased; that were illustrated with Bi^{3+}/Bi$_4$O$_7$, Bi$_2$O$_4$ and Bi$_2$O$_5$ transitions [54,55]. At the backward scan, the cathodic peak, which was observed at −0.95 V, was illustrated with the reduction of bismuth oxide species. The CV of the NiBi binary coating shows both the behaviors of Ni and Bi, which indicates the successive co-deposition of two metals. There are three anodic peaks at −0.64 V, −0.48 V and 0.45 V also two cathodic peaks at 0.33 V and −0.99 V were observed. The illustrated oxidation reactions are Ni/Ni^{2+}and Bi/Bi^{3+} at −0.64 V, −0.48 V, respectively [52–55]. At the forward scan, between the −0.40 and 0.40 V potential ranges, anodic events were illustrated with Bi^{3+}/Bi$_4$O$_7$, Bi$_2$O$_4$ and Bi$_2$O$_5$ transitions [54,55]. The Ni^{2+}/Ni^{3+} oxidation was observed at 0.45 V. At the reverse scan, Ni^{3+}/Ni^{2+} reduction was observed at 0.33 V. The peak at −0.99 V was related with the reduction of bismuth oxides. In Fig. 4 at the reverse scan, the cathodic current due to HER, increased at −1.23, −1.38 and −1.13 V for Cu/Ni, Cu/Bi and Cu/NiBi-2 electrodes respectively. This difference can be attributed with the reaction resistances or over potential values, which are inherent of the electrochemical reactions depending on the surface activities of the electrodes [14]. The current density values were 38, 3.6, 68 mA/cm^{-2} at −1.4 V for Cu/Ni, Cu/Bi and Cu/NiBi-2 respectively. For Cu/NiBi-2, the observed current increase could be explained by the decreasing the hydrogen over potential.

All electrochemical results show that, the HER activity of NiBi-2 coating was considerably higher in comparison to the nickel and other binary coatings. This activity is deeply related with the sur-

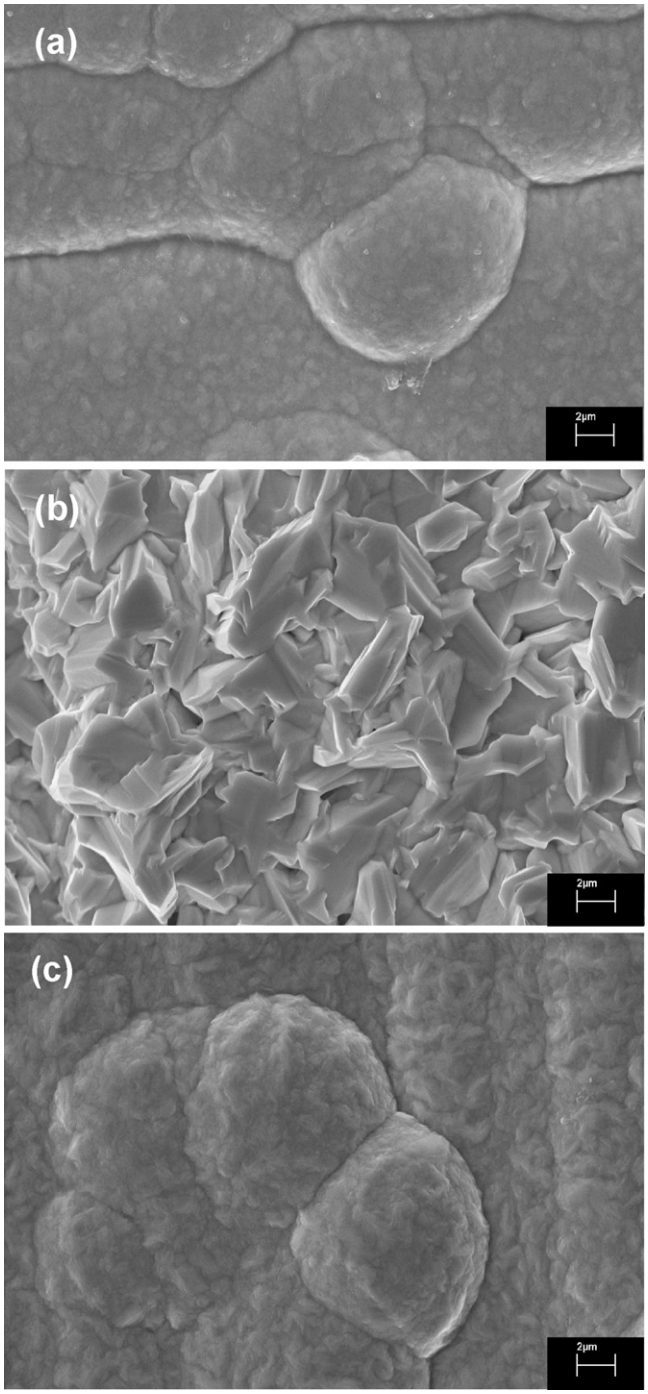

Fig. 5. SEM images of Cu/Ni (a), Cu/Bi (b), Cu/NiBi-2 (c) electrodes.

face morphology of electrodes so, SEM micrographs were analyzed. Fig. 5a shows the typical micrograph of nickel coated surface. The similar morphology was reported in the literature [30,41,52]. In Fig. 5a nodular structures were distributed on the surface. As seen in Fig. 5b, the Bi coating has significantly different crystalline structures than Ni. The agglomerates with different sizes were visible in Cu/Bi surface. In Fig. 5c, the binary coating has the characteristics of both Ni and Bi coatings. Furthermore; it is rougher than Cu/Ni surface, and leads a high surface area available for the HER. As seen, the SEM images correlate the determined EIS parameters such as n and R_f values.

Although the SEM is a powerful technique for monitoring the electrode surfaces, the quantitative components of coatings cannot be calculated with this method so, energy dispersive X-ray (EDX) technique was obtained. The results of Cu/Ni, Cu/Bi and Cu/NiBi-2 analysis was presented in Fig. 6, other analysis (all binary coatings) was summarized in Table 2. In Fig. 6a and b, only Ni and Bi peaks were shown respectively, neither Cu/Ni nor Cu/Bi analysis shows copper peaks. This means; all over the copper surface was covered and there is not any hole or crack on the electrode surface as seen from SEM images. In Fig. 6c both peaks of Ni and Bi were shown. The chemical composition of

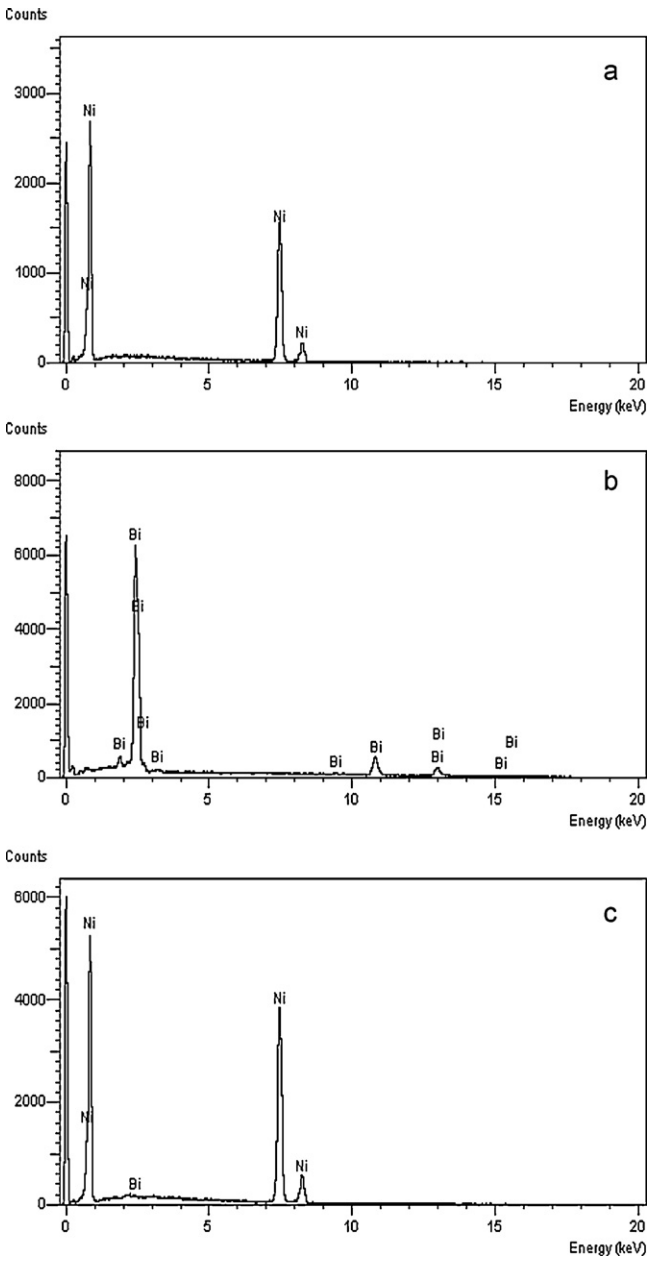

Fig. 6. EDX results of Cu/Ni (a), Cu/Bi (b), Cu/NiBi-2 (c) electrodes.

Table 2
EDX results.

Coating	Ni (%)	Bi (%)
NiBi-1	99.78	0.22
NiBi-2	99.71	0.29
NiBi-3	99.57	0.43
NiBi-4	99.51	0.49

the Cu/NiBi-2 surface was 0.29% Bi and 99.71% Ni (Table 2). The EDX results showed that the chemical composition of the coating can be changed by changing the molar ratio of Ni^{2+} and Bi^{3+} in the plating bath. Furthermore, all results show that, the chemical composition of the coatings deeply affects the catalytic activity of HER.

4. Conclusions

In this study, nickel and nickel–bismuth binary coatings with various chemical compositions were deposited on the copper electrode. In view of their possible applications as electrocatalytic materials for the HER in the alkaline media, the potentiodynamic measurements, EIS and CV techniques were obtained. The characterization was utilized with CV, SEM and EDX. Results show that the binary coatings exhibit better catalytic activity as compared to nickel. The microstructural feature of coatings and synergetic effect play a fundamental role on this efficiency. The calculated R_f values and the SEM micrographs correlate this phenomenon. The HER was occurred at lower potential values, and the charge transfer resistance values decrease on the binary coatings. In addition the activity of the coatings was depending on the chemical composition of the binary coatings. Cu/NiBi-2 was found to be the convenient cathode material under these conditions.

Acknowledgements

The authors are greatly thankful to Çukurova University Research Fund for financial support (project number: FEF2010D8).

References

[1] F. Rosalbino, S. Delsante, G. Borzone, E. Angelini, J. Alloys Compd. 429 (2007) 270–275.
[2] R. Solmaz, G. Kardaş, Electrochim. Acta 54 (2009) 3726–3734.
[3] D. Vojtecha, P. Guhlova, M. Mortanikova, P. Janík, J. Alloys Compd. 494 (2010) 456–462.
[4] W.X. Chen, Int. J. Hydrogen Energy 26 (2001) 603–608.
[5] F. Rosalbino, D. Maccio, A. Saccone, E. Angelini, S. Delfino, J. Alloys Compd. 431 (2007) 256–261.
[6] E. Rasten, G. Hagen, R. Tunold, Electrochim. Acta 48 (2003) 3945–3952.
[7] W. Hu, X. Cao, F. Wang, Y. Zhang, Int. J. Hydrogen Energy 22 (1997) 441–443.
[8] R.F. Susanti, A. Nugroho, J. Lee, Y. Kim, J. Kim, Int. J. Hydrogen Energy 36 (2011) 3895–3906.
[9] B. Acharya, A. Dutta, P. Basu, Int. J. Hydrogen Energy 35 (2010) 1582–1589.
[10] M.D. Merrill, B.E. Logan, J. Power Sources 191 (2009) 203–208.
[11] A. Giordano, C. Cantu, A. Spagni, Bioresour. Technol. 102 (2011) 4474–4479.
[12] G. Sheela, M. Pushpavanam, S. Pushpavanam, Int. J. Hydrogen Energy 27 (2002) 627–633.
[13] Z.D. Wei, M.B. Ji, S.G. Chen, Y. Liu, C.X. Sun, G.Z. Yin, P.K. Shen, S.H. Chan, Electrochim. Acta 52 (2007) 3323–3329.
[14] K. Zeng, D. Zhang, Prog. Energy Combust. Sci. 36 (2010) 307–326.
[15] R.F. De Souza, J.C. Padilha, R.S. Goncalves, M.O. De Souza, J.R. Berthelot, J. Power Sources 164 (2007) 792–798.
[16] R.F. De Souza, G. Loget, J.C. Padilha, E.M.A. Martini, M.O. De Souza, Electrochem. Commun. 10 (2008) 1673–1675.
[17] H. Agustos, Z. Utlu, O. Kıncay, Nuclear and Renewable Energy Sources Conference with International Participation, Ankara, Turkey, 2009, pp. 301–308.
[18] M. Fichtner, J. Alloys Compd. (2011), doi:10.1016/j.jallcom.2010.12.179, in press.
[19] Y. Zhu, C. Yang, J. Zhu, L. Li, J. Alloys Compd. 509 (2011) 5309–5314.
[20] Y. Zhang, B. Li, H. Rena, X. Ding, X. Liu, L. Chen, J. Alloys Compd. 509 (2011) 2808–2814.
[21] K. Young, R. Regmi, G. Lawes, T. Ouchi, B. Reichman, M.A. Fetcenko, A. Wu, J. Alloys Compd. 490 (2010) 282–292.
[22] R. Solmaz, A. Döner, Gülfeza Kardaş, Electrochem. Commun. 10 (2008) 1909–1911.
[23] B. Campillo, P.J. Sebastian, S.A. Gamboa, J.L. Albarran, L.X. Caballero, Mater. Sci. Eng. C 19 (2002) 115–118.
[24] M. Jafariana, O. Azizi, F. Gobal, M.G. Mahjani, Int. J. Hydrogen Energy 32 (2007) 1686–1693.
[25] E. Irissou, M. Blouin, L. Roue, J. Huot, R. Schulz, D. Guay, J. Alloys Compd. 345 (2002) 228–237.
[26] N.V. Krstajic, V.D. Jovic, Lj.G. Krstajic, B.M. Jovic, A.L. Antozzi, G.N. Martelli, Int. J. Hydrogen Energy 33 (2008) 3676–3687.
[27] F.C. Crnkovic, S.A.S. Machado, L.A. Avaca, Int. J. Hydrogen Energy 29 (2004) 249–254.
[28] M. Azzag, M. Chatelut, O. Vittori, J. Appl. Electrochem. 27 (1997) 699–705.
[29] N. Jiang, H.M. Meng, L.J. Song, H.Y. Yu, Int. J. Hydrogen Energy 35 (2010) 8056–8062.
[30] C. Cai, X.B. Zhu, G.Q. Zheng, Y.N. Yuan, X.Q. Huang, F.H. Cao, J.F. Yang, Z. Zhang, Surf. Coat. Technol. 205 (2011) 3448–3454.
[31] J.K. Lee, Y. Yi, H.J. Lee, S. Uhm, J. Lee, Catal. Today 146 (2009) 188–191.
[32] M.A. Garcia-Contreras, S.M. Fernandez-Valverde, J.R. Vargas-Garcia, J. Alloys Compd. 504S (2010) S425–S428.
[33] M.P.M. Kaninski, V.M. Nikolic, G.S. Tasic, Z.Lj. Rakocevic, Int. J. Hydrogen Energy 34 (2009) 703–709.
[34] R. Solmaz, A. Döner, İ. Şahin, A.O. Yüce, G. Kardaş, B. Yazıcı, M. Erbil, Int. J. Hydrogen Energy 34 (2009) 7910–7918.
[35] M. Yang, Z. Hu, J. Electroanal. Chem. 583 (2005) 46–55.
[36] E. Hark, K. Lust, A. Janes, E. Lust, J. Solid State Electrochem. 13 (2009) 745–754.
[37] R. Pauliukaite, S.B. Hocoeevar, B. Ogorevc, J. Wang, Electroanalysis 16 (2004) 719–723.
[38] T. Romann, E. Lust, Electrochim. Acta 55 (2010) 5746–5752.
[39] S. Ham, S. Jeon, M. Park, S. Choi, K. Paeng, N. Myung, K. Rajeshwar, J. Electroanal. Chem. 638 (2010) 195–203.
[40] F. Rosalbino, D. Maccio, E. Angelini, A. Saccone, S. Delfino, J. Alloys Compd. 403 (2005) 275–282.
[41] E. Navarro-Flores, Z. Chong, S. Omanovic, J. Mol. Catal. A: Chem. 226 (2005) 179–197.
[42] R.K. Shervedani, A.R. Madram, Int. J. Hydrogen Energy 33 (2008) 2468–2476.
[43] R.K. Shervedani, A. Lasia, J. Appl. Electrochem. 29 (1999) 979–986.
[44] D. Risovic, S.M. Poljac, K. Furic, M. Gojo, Appl. Surf. Sci. 255 (2008) 3063–3070.
[45] T. Pajkossy, Solid State Ionics 176 (2005) 1997–2003.
[46] I. Herraiz-Cardona, E. Ortega, V. Perez-Herranz, Electrochim. Acta 56 (2011) 1308–1315.
[47] A. Altube, A.R. Pierna, F.F. Marzo, J. Non-Cryst. Solids 287 (2001) 297–301.
[48] J. Fleig, J. Maier, Solid State Ionics 94 (1997) 199–207.
[49] M.M. Jaksic, Int. J. Hydrogen Energy 26 (2001) 559–578.
[50] M.M. Jaksic, Solid State Ionics 136–137 (2000) 733–746.
[51] A. Takasaki, T. Homma, J. Alloys Compd. 340 (2002) 127–131.
[52] M.A. Abdel Rahim, R.M. Abdel Hameed, M.W. Khalil, J. Power Sources 134 (2004) 160–169.
[53] Z. Grubac, Z. Petrovic, J. Katic, M. Metikos-Hukovic, R. Babic, J. Electroanal. Chem. 645 (2010) 87–93.
[54] V. Vivier, A. Regis, G. Sagon, J.Y. Nedelec, L.T. Yu, C.C. Vivier, Electrochim. Acta 46 (2001) 907–914.
[55] I. Svancara, L. Baldrianova, E. Tesarova, S.B. Hocevar, S.A.A. Elsuccary, A. Economou, S. Sotiropoulos, B. Ogorevc, K. Vytras, Electroanalysis 18 (2006) 177–185.